

Flux state and anomalous quantum Hall effect in the square double-exchange model

 Xiao Chen,¹ Shuai Dong,² and J.-M. Liu^{1,3}
¹Laboratory of Solid State Microstructures, Nanjing University, Nanjing 210093, China

²Department of Physics, Southeast University, Nanjing 211189, China

³International Center for Materials Physics, Chinese Academy of Sciences, Shenyang 110016, China

(Received 18 January 2010; revised manuscript received 28 January 2010; published 19 February 2010)

The anomalous Hall effect (AHE) around the flux state in square double-exchange model is investigated. By introducing the lattice distortion and local chirality, the system can break the parity symmetry and time-reversal symmetry spontaneously, and thus generate a topological nontriviality in the band structure associated with the AHE. Moreover, a possible realization of this AHE in multiferroic TbMnO₃ is discussed.

 DOI: [10.1103/PhysRevB.81.064420](https://doi.org/10.1103/PhysRevB.81.064420)

PACS number(s): 75.10.Jm, 75.30.Mb, 75.47.Lx

In condensed matters, novel spin orders often lead to novel physical phenomena. For instance, some multiferroics have a spiral spin order which breaks the spatial inversion symmetry and gives rise to ferroelectric polarization, origin of which is completely different from conventional ferroelectricity.^{1,2} This spiral spin order can be scaled by a vector spin chirality (VSC) $\mathbf{S}_i \times \mathbf{S}_j$ and has become an important concept in the physics of spin current and spin liquid.^{3,4} Besides the VSC, there is another scalar spin chirality defined by

$$\chi_{ijk} = \mathbf{S}_i \cdot (\mathbf{S}_j \times \mathbf{S}_k), \quad (1)$$

which breaks the parity (P) and time-reversal (T) symmetry and was first proposed by Wen *et al.*⁵ It is clear that chirality χ would be nonzero for a noncoplanar spin order.

On the other hand, recent studies showed that the noncoplanar spin order is relevant to the intrinsic anomalous Hall effect (AHE) observed in double-exchange system, in which the noncoplanar background spin texture acts as a gauge field for itinerant electrons propagating in the lattice.⁶⁻¹⁵ Generally speaking, the intrinsic AHE has the topological origin and can be characterized by the Berry phase and Chern number. To manifest this mechanism, the system should break the P symmetry and T symmetry spontaneously and simultaneously.^{15,16} For a double-exchange model, the T symmetry can be violated for those spin configurations with the local spin chirality, while the P symmetry can be broken in some geometrically frustrated lattices. For instance, Ohgushi *et al.*⁶ once discussed the AHE on kagome lattice where a finite local spin chirality in the three-site unit cell can generate nonzero Hall conductance. This model has been extended to other geometrically frustrated systems such as the three-dimensional (3D) pyrochlore lattice.⁷⁻⁹ Therefore, a geometrically frustrated lattice with spin chirality would be of significance in terms of AHE physics.

Unfortunately, the square lattice usually has no geometrically frustrated structure, and thus it is not easy to violate the P symmetry since the chiralities on adjacent plaquettes tend to cancel each other due to the lattice symmetry and thus the AHE becomes hard to realize in the square lattice. However, the square lattice (and its distorted forms) takes up the majority in the practical transitional metals' oxides such as colossal magnetoresistance manganites¹⁷ and Fe-based pnictide superconductors.¹⁸ Besides, the realization of AHE on

the square lattice is also fundamentally important and physically interesting.^{19,20}

In this paper, the AHE on the square lattice is realized theoretically by introducing two mechanisms to break the P symmetry. One is to induce some lattice distortions which can lead to the change in hopping amplitude of itinerant electrons. The other is to construct a special unit cell which breaks the P symmetry. These two mechanisms are different from the previous considered spin-orbit interaction (SOI) which can directly generate topological nontriviality in the band structure and associate with the AHE.^{15,16,21} Our discussion will be primarily restricted to a "flux" state at the half filling of one-orbital double-exchange model. We hope that these two mechanisms can be alternating approaches (other than the SOI mechanism) to the AHE in the square lattice and eventually realized in some real materials.

The Hamiltonian of one-orbital double-exchange model on the two-dimensional square lattice can be written as¹⁷

$$H = - \sum_{\text{NN}} t_1 c_{i,\sigma}^\dagger c_{j,\sigma} - \sum_{\text{NNN}} t_2 c_{i,\sigma}^\dagger c_{k,\sigma} - J_H \sum_i \mathbf{S}_i \cdot c_{i,\alpha}^\dagger \sigma_{\alpha\beta} c_{i,\beta} + J_1 \sum_{\text{NN}} \mathbf{S}_i \cdot \mathbf{S}_j + J_2 \sum_{\text{NNN}} \mathbf{S}_i \cdot \mathbf{S}_j, \quad (2)$$

where the first term describes the electron hopping between the nearest-neighbor (NN) sites and the hopping amplitude t_1 is taken as the energy unit. The second term is the electron hopping between the next-nearest-neighbor (NNN) sites. In the following, t_2 is arbitrarily set as 0.25 as an example, since the AHE result is qualitatively independent of its exact value as long as it is nonzero, which will be further discussed below. The third term is the Hund coupling linking the itinerant electrons with the background spins \mathbf{S} (assumed classical and normalized as $|\mathbf{S}|=1$) where J_H is the coupling factor. The last two terms are the antiferromagnetic superexchanges between the background spins with J_1 and J_2 as the coefficients for the NN and NNN sites, respectively. This model has been extensively investigated for various transitional metals' oxides, and more details of this model can be found in Ref. 17.

For the third term, by applying a canonical transformation, the Hamiltonian can be simplified by adopting the site-dependent spin-polarization axis. In the $J_H \rightarrow \infty$ limit, the spin of the hopping electron is forced to align parallel to the

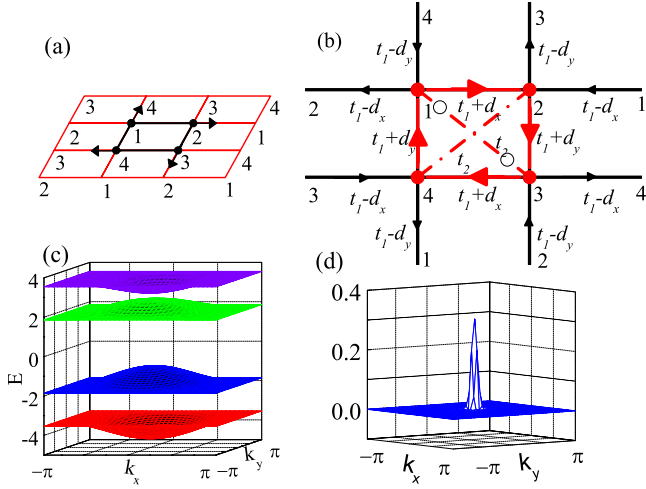


FIG. 1. (Color online) (a) The flux state with the four-site unit cell. (b) The lattice is distorted with atoms 1 and 3 moving in reversed direction with the new positions shown as open circles. The NN hopping amplitude t_1 is varied correspondingly. The arrows on bonds indicate the signs of the phases of the t_{ij}^{eff} . (c) The band structure of Eq. (4) with the parameters sets $t_{r1}=1$, $t_{r2}=0.25$, $d=1$, and $\phi=\pi/6$. (d) Gauge flux density of the third band of (c).

on-site \mathbf{S} , and thus the hopping terms in the Hamiltonian can be transferred into the form $t_{ij}^{eff} c_i^\dagger c_j$, with the effective hopping integral

$$t_{ij}^{eff} = t \left[\cos \frac{\theta_i}{2} \cos \frac{\theta_j}{2} + \sin \frac{\theta_i}{2} \sin \frac{\theta_j}{2} e^{-i(\varphi_i - \varphi_j)} \right] = t e^{i\varphi_{ij}} \cos \frac{\theta_{ij}}{2}, \quad (3)$$

where t can be t_1 or t_2 . θ and φ are the polar coordinates of spin \mathbf{S} . The phase factor φ_{ij} can be viewed as the gauge vector potential and θ_{ij} is the angle between \mathbf{S}_i and \mathbf{S}_j .⁶ When the itinerant electrons move along a closed loop, they can feel the induced gauge flux which is indistinguishable from the magnetic flux. This gauge flux is related to the spin chirality and leads to the AHE.^{6,9,14,15}

For this model, the ground state can be calculated with the variational method, namely, by comparing the ground-state energies of several preset spin configurations. Around half filling, when the $J_1=J_2>0.15$, the ground state is the flux state. This state has four sites in the unit cell, as shown in Fig. 1(a). In one plaquette, the neighboring background spins are perpendicular to each other. When an itinerant electron travels around the plaquette, it can acquire an additional π flux. In fact, this flux state was reported earlier in some similar systems.^{22,23} The flux phase can have many degenerate states by shifting and rotating the spin structures. Thus, a specific state, with $(\mathbf{S}_1, \mathbf{S}_3)$ along the y axis and $(\mathbf{S}_2, \mathbf{S}_4)$ along the x axis, will be adopted in the following study, which forms a spin order in the x - y plane. In practical calculation, to remove the degeneration and stabilize this state, a small anisotropic energy $H_2 = \sum K_\alpha S_\alpha^2$ (subscript $\alpha=1-4$, $K_1=K_3=-0.02$, and $K_2=K_4=0.02$) is also considered, which favors $(\mathbf{S}_1, \mathbf{S}_3)$ along the y axis and $(\mathbf{S}_2, \mathbf{S}_4)$ in the x - z plane. In fact, the flux state is with coplanar spin order and the AHE

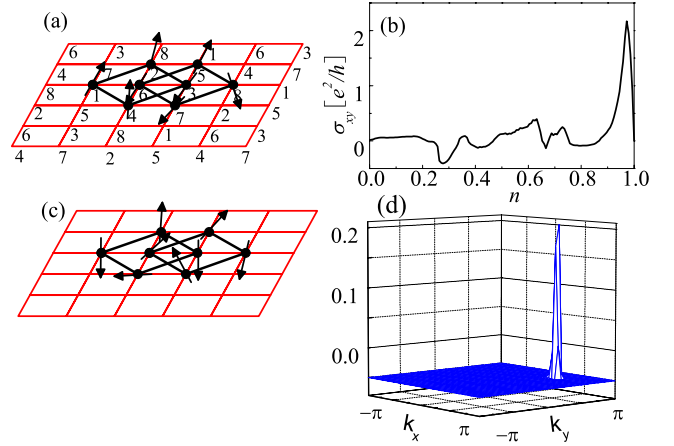


FIG. 2. (Color online) (a) The ground state with the parameter sets $J_1=J_2=0.04$, $J_3=0.025$, $t_1=1$, $t_2=0.25$, $d=0.4$, and $n=0.5$. The unit cell expands to eight site here. (b) The Hall conductance as a function of the conduction electron density n with the spin order shown in (a). This result is calculated by Eq. (8). (c) An example of the nontrivial spin order in the special eight-site unit cell. (d) Gauge flux density $\mathbf{B}(k)$ of the first band with the spin order shown in (c).

conductance is forbidden. Therefore, additional contributions should be included for allowing the AHE.

In real materials, due to the ionic size mismatch or competing exchange interactions, the square lattice would be distorted more or less. For instance, in multiferroic RMnO_3 , the Mn-O-Mn chain is distorted in noncentrosymmetric manners caused by the Dzyaloshinsky-Moriya (DM) interaction, giving rise to the staggered Mn-O-Mn angles.^{1,25} For simplicity, a simple lattice distortion mode is adopted, as shown in Fig. 1(b), where the first and third cations are displaced from the original positions along the opposite directions. Due to the x - y symmetry, the cation displacement along x and y are assumed to be the same. In a first-order approximation, the corresponding hopping amplitude varies linearly with the tiny lattice distortion, and thus the NN hopping amplitude $t'_1=t_1 \pm d$, where d is the tiny amendment caused by the distortion. The influence to the NNN hopping amplitude t_2 is not considered because the exact value of NNN hopping is not qualitatively important to obtain the AHE. Take one chain of the lattice, for example, the hopping amplitude becomes staggeringly ordered and the P symmetry of the lattice is broken.

In this P-symmetry broken configuration, if the spin order may be not exactly confined in the x - y plane, i.e., spins \mathbf{S}_1 and \mathbf{S}_3 tilt slightly from the y axis and are not parallel to each other. Therefore, the local spin order may become noncoplanar with each plaquette having a gauge flux penetrating it. In this condition, the NN hopping can be approximately modified to the following form: $t_{ij}^{eff} = t_{r1} e^{i\varphi_{ij}}$ with t_{r1} the renormalized NN hopping amplitude.⁶ We take $\varphi_{ij} = \phi$ for the hopping direction along the arrow direction while $\varphi_{ij} = -\phi$ opposite to the arrow direction as shown in Fig. 2(b). In the flux state, $\varphi_{ij} = \pm \pi/4$, while for the noncoplanar spin order case, ϕ deviates from $\pi/4$.⁶ In addition, the renormalized NNN hopping amplitude is set as a real constant t_{r2} for simplicity. The Hamiltonian matrix for this model can be written in the momentum space,

$$H(k) = \begin{pmatrix} 0 & e^{i\phi}f_1 & f_3 & e^{-i\phi}f_2 \\ e^{-i\phi}f_1^* & 0 & e^{i\phi}f_2 & f_3 \\ f_3 & e^{-i\phi}f_2^* & 0 & e^{i\phi}f_1^* \\ e^{i\phi}f_2^* & f_3 & e^{-i\phi}f_1 & 0 \end{pmatrix}, \quad (4)$$

where $f_1(k) = t_{r1} \cos(k_x/2) + id \sin(k_x/2)$, $f_2(k) = t_{r1} \cos(k_y/2) + id \sin(k_y/2)$, and $f_3(k) = t_{r2} [\cos[(k_x - k_y)/2] + \cos[(k_x + k_y)/2]]$. Now, the AHE conductance can be calculated. The contribution to the AHE conductance from each band is written as,^{6,16}

$$\begin{aligned} \sigma_{xy}^n &= \frac{e^2}{h} \frac{1}{2\pi i} \int_{BZ} d^2k \mathbf{z} \cdot \nabla_k \times \mathbf{A}_n(k) \\ &= \frac{e^2}{h} \frac{1}{2\pi i} \int_{BZ} d^2k \mathbf{z} \cdot \mathbf{B}_n(k) = \frac{e^2}{h} C_n, \end{aligned} \quad (5)$$

where $\mathbf{A}_n(\mathbf{k}) = \langle nk | \nabla | nk \rangle$ is the vector potential defined with the n th wave function, $\mathbf{B}_n(\mathbf{k})$ is the gauge flux density, and C is the so-called first Chern number. At $d=0$ case, namely, the ideal square lattice without any distortion, the P symmetry is maintained, leading to zero Chern number for each band. At $d \neq 0$ case, the P symmetry is broken. Around $\phi = \pi/4$, $C = [0, 0, 1, -1]$ at $\phi < \pi/4$, and $C = [1, -1, 0, 0]$ at $\phi > \pi/4$ (at $\phi = \pi/4$, the T symmetry is conserved with $C=0$ for each band). For instance, at $\phi = \pi/6$, the band structure is shown in Fig. 1(c), and the gauge flux density $\mathbf{B}(\mathbf{k})$ of the third band is shown in Fig. 1(d).

For Hamiltonian Eq. (2), the nonzero NNN hopping term is essentially important to generate the topological nontriviality in the band structure. This can be intuitively understood as follows. For Eq. (4), in the large d limit, $f_1(k) \approx id \sin(k_x/2)$, under the transformation $UHU^T \rightarrow H'$ (U is a real constant matrix),²⁴ the Hamiltonian matrix Eq. (4) can be further decoupled into the form

$$H' = \begin{pmatrix} h_1(k) & 0 \\ 0 & h_2(k) \end{pmatrix}, \quad (6)$$

where $h_1(k)$ and $h_2(k)$ are both 2×2 matrixes.

For the matrix $h_1(k)$, around $k = (\pi, \pi)$, the electron can be considered as a generalized Dirac fermion and the effective Hamiltonian $h_1(k)$ ($h_2(k)$ can be treated in a similar way) is

$$h_1(k) = -\frac{t_{r2}}{2} k'_x k'_y \sigma^x + \frac{d \cos \theta}{8} (k_y'^2 - k_x'^2) \sigma^y + 2d \sin \phi \sigma^z, \quad (7)$$

where $k'_x \equiv k_x - \pi$ and $k'_y \equiv k_y - \pi$. The general form of Eq. (7) was thoroughly addressed in Ref. 16 and the corresponding Chern number for the upper and lower bands is $C = \pm 2 \text{sgn}(t_{r2}/d)$ (at $\phi = \pi/6$). If $t_{r2} = 0$, $C = 0$ for both bands, indicating that the NNN hopping term is indispensable in generating the Hall conductance.

Consequently, one can argue that the lattice distortion provides an effective method to break the P symmetry, and yet a noncoplanar spin order as the ground state is still required to generate AHE conductance. In fact, the noncoplanar spin order can be accomplished by further taking into account the frustrated interaction. For instance, by

adding the third-neighbor (3rd N) superexchange interaction $H_3 = \sum_{3\text{rd N}} J_3 \mathbf{S}_i \cdot \mathbf{S}_j$ to the distorted double-exchange model described by Eq. (2), the competition between H_1 , H_2 , and H_3 will lead to a noncoplanar spin order. In this condition, the original flux state at the half filling evolves into a state as shown in Fig. 2(a). The unit cell expands to eight site and is formed with two interlaced square sublattices compared with the original four-site unit cell (formed by \mathbf{S}_6 , \mathbf{S}_3 , \mathbf{S}_7 , and \mathbf{S}_4). For this spin configuration, we can straightly calculate the Hall conductivity at zero temperature by using the Kubo formula¹⁶

$$\sigma_{xy} = \frac{e^2}{h} \frac{1}{2\pi i} \sum_{nmk} \frac{\langle nk | J_x | mk \rangle \langle mk | J_y | nk \rangle - \text{H.c.}}{[\varepsilon_n(k) - \varepsilon_m(k)]^2}, \quad (8)$$

where $|nk\rangle$ is the occupied state and $|mk\rangle$ is the empty state. J_x (J_y) is the x (y) components of the current operator. The calculation is performed in momentum space with the summation over all the eight bands. For example, with a finite J_3 [see Fig. 2(a)'s caption], $\sigma_{xy} = 0.13e^2/h$ at half filling, clearly indicating that this ground state does exhibit the AHE. Besides, the Hall conductance as the function of conduction electron density n is shown in Fig. 2(b), with the spin configuration fixed as Fig. 2(a). The curve in Fig. 2(b) fluctuates dramatically, showing that the AHE is sensitive to n .²¹

Interestingly, additional investigation of the ground state in Fig. 2(a) indicates that besides the lattice distortion, this special unit cell structure also breaks the P symmetry spontaneously. This is because that in the eight-site unit cell, the left and right sites of each site could be different. Thus for this unit cell structure, with the local spin chirality, the band structure can lead to nonzero Chern number and Hall conductance even without any lattice distortion or NNN hopping. For the local spin order shown in Fig. 2(c), the eight bands are topologically nontrivial and the corresponding Chern number $C = [1, -1, 0, 0, 0, 0, -1, 1]$, with the gauge flux density of the first band shown in Fig. 2(d). In fact, due to the frustrated magnetic interaction, the unit cell could involve more sites and become even larger with the parity violation satisfied. For instance, for Eq. (2), with large J_1 ($J_2 = J_1$) and low n , the variational calculation indicates the ground state is with the coplanar spiral order. This coplanar spiral order can evolve into the 3D spiral order by including the H_2 and H_3 term. However, in this case, the unit cell also expands dramatically, and the band calculation becomes much more challenging. An alternative path to solve this problem is to take the calculation in the real space. For instance, Yi *et al.* did this real-space calculations to interpret the AHE observed in 3D chiral ferromagnet MnSi, where the complex magnetic interaction leads to the Skyrmion structure.¹⁰⁻¹² The ground state we address here seems to be a special case with a relatively small unit cell.

Although the calculation of Eq. (2) and the addressed two mechanisms are more or less theoretically oriented, their realization in real systems is still possible. For example, multiferroic TbMnO₃ is a promising candidate to illustrate these two mechanisms and observe the AHE. In TbMnO₃, besides the GeFeO₃-type distortion, which forms the Mn-O-Mn

zigzag chain, the DM interaction is also present.²⁵ In this case, due to the spiral order of the background spin, the Mn-O-Mn zigzag chain is distorted with all the oxygen ions displaced in the same direction.²⁵ Therefore the adjacent Mn-O-Mn angles are different, leading to the staggered order of the effective Mn-Mn hopping amplitude and broken parity symmetry. For TbMnO₃, neutron-scattering experiments confirmed that the background t_{2g} electrons form a coplanar spiral order. To excite the noncoplanar spin order, a magnetic field with its direction different from the spin order plane can be applied, allowing the nonzero Hall conductance. In addition, the ferroelectric polarization in TbMnO₃ aligns along the direction of $\mathbf{e}_{ij} \times (\mathbf{S}_i \times \mathbf{S}_j)$. Therefore, the noncollinear ferroelectric polarization should be expected for this noncoplanar spin order. Moreover, the Tb³⁺ cations can be doped by other +4 cations, which can modulate the itinerant electrons density and directly control the AHE.²¹ However, for

these calculations, a more practical two-orbital double-exchange model should be employed.

In conclusion, we have studied the double-exchange model on a square lattice with frustrated superexchange interactions. The calculated nonzero Hall conductance is attributed to two distinct mechanisms, one is the lattice distortion and the other is the locally nontrivial spin order. Both of these mechanisms break the P symmetry and can generate the AHE spontaneously.

The authors acknowledge E. Dagotto, Q. H. Wang, N. Nagaosa, and R. Shindou for fruitful discussions. This work was supported by the National Nature Science Foundation of China (Grants No. 50832002 and No. 10874075), the National Key Projects for Basic Researches of China (Grants No. 2006CB921802 and No. 2009CB929501), and the Nature Science Foundation of Jiangsu Province, China (Grant No. BK2008024).

¹T. Kimura, *Annu. Rev. Mater. Res.* **37**, 387 (2007).

²K. F. Wang, J.-M. Liu, and Z. F. Ren, *Adv. Phys.* **58**, 321 (2009).

³H. Katsura, N. Nagaosa, and A. V. Balatsky, *Phys. Rev. Lett.* **95**, 057205 (2005).

⁴J. H. Park, S. Onoda, N. Nagaosa, and J. H. Han, *Phys. Rev. Lett.* **101**, 167202 (2008).

⁵X. G. Wen, F. Wilczek, and A. Zee, *Phys. Rev. B* **39**, 11413 (1989).

⁶K. Ohgushi, S. Murakami, and N. Nagaosa, *Phys. Rev. B* **62**, R6065 (2000).

⁷R. Shindou and N. Nagaosa, *Phys. Rev. Lett.* **87**, 116801 (2001).

⁸I. Martin and C. D. Batista, *Phys. Rev. Lett.* **101**, 156402 (2008).

⁹Y. Taguchi, Y. Oohara, H. Yoshizawa, N. Nagaosa, and Y. Tokura, *Science* **291**, 2573 (2001).

¹⁰A. Neubauer, C. Pfleiderer, B. Binz, A. Rosch, R. Ritz, P. G. Niklowitz, and P. Boni, *Phys. Rev. Lett.* **102**, 186602 (2009).

¹¹M. Lee, W. Kang, Y. Onose, Y. Tokura, and N. P. Ong, *Phys. Rev. Lett.* **102**, 186601 (2009).

¹²S. D. Yi, S. Onoda, N. Nagaosa, and J. H. Han, *Phys. Rev. B* **80**, 054416 (2009).

¹³K. Taguchi and G. Tatara, arXiv:0811.0890 (unpublished).

¹⁴S. Onoda and N. Nagaosa, *Phys. Rev. Lett.* **90**, 196602 (2003).

¹⁵N. Nagaosa, J. Sinova, S. Onoda, A. H. MacDonald, and N. P. Ong, arXiv:0904.4154 (unpublished).

¹⁶M. Onoda and N. Nagaosa, *J. Phys. Soc. Jpn.* **71**, 19 (2002).

¹⁷E. Dagotto, T. Hotta, and A. Moreo, *Phys. Rep.* **344**, 1 (2001).

¹⁸Y. Kamihara, T. Watanabe, M. Hirano, and H. Hosono, *J. Am. Chem. Soc.* **130**, 3296 (2008).

¹⁹N. Goldman, A. Kubasiak, P. Gaspard, and M. Lewenstein, *Phys. Rev. A* **79**, 023624 (2009).

²⁰N. Goldman, A. Kubasiak, A. Bermudez, P. Gaspard, M. Lewenstein, and M. A. Martin-Delgado, *Phys. Rev. Lett.* **103**, 035301 (2009).

²¹K. S. Takahashi, M. Onoda, M. Kawasaki, N. Nagaosa, and Y. Tokura, *Phys. Rev. Lett.* **103**, 057204 (2009).

²²M. Yamanaka, W. Koshibae, and S. Maekawa, *Phys. Rev. Lett.* **81**, 5604 (1998).

²³D. F. Agterberg and S. Yunoki, *Phys. Rev. B* **62**, 13816 (2000).

²⁴This approximation is not accurate especially at $k_x=0$. We take this approximation here just to emphasize the importance of t_{r2} .

²⁵T. Arima, A. Tokunaga, T. Goto, H. Kimura, Y. Noda, and Y. Tokura, *Phys. Rev. Lett.* **96**, 097202 (2006).